HiSST: 3rd International Conference on
High-Speed Vehicle Science Technology
14 -19 April 2024, Busan, Korea

Development of a Dual-Layer Ablator for Spacecraft Heat Shield Applications

Rajesh Kumar Chinnaraj[1], Young Chan Kim[1], Seong Man Choi[1,]*

Abstract

For spacecraft heat shield applications, we have developed a dual-layer carbon-phenolic/silica phenolic ablator. The development of this dual-layer ablator began with testing a carbon-phenolic material with two different lamination angles of 0° and 30°, using a high-velocity oxygen fuel (HVOF) material ablation test facility. Based on HVOF results, the 30° carbon-phenolic material is selected as the recession layer for the dual-layer ablator. The 30° carbon-phenolic material was augmented with a silica-phenolic material (used as the insulating layer) and tested in a 0.4 MW supersonic arc-jet plasma wind tunnel. In plasma wind tunnel tests, dual-layer ablator specimens with varying thicknesses of carbon-phenolic layers and different surface shapes (flat-faced and hemispherical-faced) were tested. The plasma wind tunnel tests showed the specimen silica-phenolic recession layer internal temperatures were well below the set design limit of 453.15 K (180 °C). The surface temperatures of the hemispherical-faced specimens measured around 3000 K, approximately 350 K higher than those of the flat-faced specimens, leading to elevated internal temperatures. The results showed that hemispherical-faced specimens exhibited approximately 1.4 times greater recession and mass loss compared to the flat-faced specimens.

Keywords : *thermal protection system, spacecraft heat shield, ablative materials, carbon phenolic, silica phenolic*

Nomenclature

CPBAM – carbon–phenolic-based ablative material
CP – carbon-phenolic
HVOF – high-velocity oxygen fuel
JBNU – Jeonbuk National University
MC-CFRP – MUSES-C carbon fiber-reinforced polymer
PWT – plasma wind tunnel
SPOF – single point of failure
TC – thermocouple
TPS– thermal protection system

1. Introduction

During atmospheric re-entries, thermal protection systems (TPS) or heat shields are used to protect spacecraft from extreme heat loads. These extreme heat loads arise as atmospheric drag and aerodynamic heating cause air flows surrounding re-entering spacecraft to dissociate and ionize, forming high thermal plasma flows. TPS is considered as a single-point-of-failure (SPOF) subsystem for a spacecraft [1], indicating that the failure of the TPS would result in a complete mission failure. TPS and their constituent materials are generally classified into two broad categories, 1. Reusable, non-ablative, and non-charring; 2. non-reusable and ablative, including charring (non-melting) and non-charring (melting) subtypes [2].

Reusable TPS materials are typically used for low Earth orbit re-entries, where low heat flux conditions are expected. Generally, these materials absorb a significant amount of incident heat load, and as a

[1] *Department of Aerospace Engineering, Jeonbuk National University, Jeonju, Republic of Korea*
** Corresponding author, email: csman@jbnu.ac.kr*

result, they are sometimes referred to as 'heat soak' TPS. The TPS tiles and RCC materials used in NASA's space shuttles are classical examples of reusable TPS [3].

Among the non-reusable TPS materials or ablators, charring ablators are the most preferred for interplanetary spacecraft heat shield applications; all NASA interplanetary space missions so far have employed charring ablators [1]. Typical charring ablators contain organic resins, such as phenolic, reinforced using solid-phase constituents [4]. When exposed to thermal loads, the thermal degradation, i.e., the pyrolysis of the phenolic resin, is an endothermic process that absorbs a part of the incident thermal load. Also, during the pyrolysis of the phenolic resin, the resulting gases rising to the ablating surface create a blockage effect that further aids in reducing the thermal load transferred to the ablator's surface. For these reasons, phenolic-based charring ablators are most preferred for interplanetary spacecraft heat shield applications, when compared to other TPS materials.

For interplanetary Earth return space missions, carbon-phenolic-based ablative materials (CPBAMs) are the most commonly used phenolic-based charring ablators. Examples of CPBAMs are PICA, used for the Stardust Wild 2 comet mission [5]; and MC-CFRP, used for the Hayabusa Itokawa asteroid mission [6]. The constituent material properties and their structural arrangement define the overall thermal property of a carbon-phenolic material, which can be customized to meet the specific requirements of an application. So, it is very important to conduct thorough investigations of carbon-phenolic materials to understand the various thermal properties before employing them as heat shield ablators. Although carbon-phenolic materials demonstrate excellent ablative properties, they are regarded as poor thermal insulators [1]. Despite their poor thermal insulation, attributed to good thermal conductivity, carbon-phenolic materials are used in electronic components to enhance heat dissipation [7]. On the other hand, for spacecraft heat shield applications, the poor thermal insulation is unfavorable. It becomes important to improve the thermal insulation properties of the TPS materials to safeguard the metallic frame of a spacecraft during re-entry; the most common high-temperature resistant aluminum alloys begin to lose their strength when the temperature exceeds ~473 K (i.e., 200 °C) [8]. So, essentially, spacecraft heat shields are designed to maintain their back face temperatures below ~473 K (i.e., 200 °C) during re-entry to prevent any loss in the structural strength of the spacecraft's metallic frame due to the extreme forces experienced during the re-entry phase. To maintain the heat shield's back face temperature limit, a TPS material with poor thermal insulation will lead to a thicker heat shield, thereby increasing the overall mass of the spacecraft.

In CPBAM heat shields, the overall thermal insulation of the carbon-phenolic material can be enhanced by reducing the material density. This reduction in density, in turn, lowers thermal conductivity, thereby improving the thermal insulation properties. This can be achieved by altering the material's internal microstructures and composition. However, this process also results in a decrease in the material's strength [9]. This method of thermal insulation improvement demands a meticulous understanding of the carbon-phenolic material properties, but most current methods for measuring carbon-phenolic properties are considered outdated and require new measurement techniques [10].

Another way to enhance the overall thermal insulation of the CPBAM heat shield is by adding a secondary insulating layer with lower thermal conductivity to a primary flow-facing recession layer [11].

Here, we discuss the testing and development process of a dual-layer ablator based on carbon-phenolic material intended for use in a future reentry space capsule named "Space Challenge Reentry Capsule". [12]. For this spacecraft, a design limit is set with a nominal heat shield back face temperature value of 453.15 K (180 °C).

Firstly, JBNU's high-velocity oxygen fuel (HVOF) material ablation test facility was used to test the carbon-phenolic material with two lamination angles of 0° and 30°. Based on the results, the carbon-phenolic material with 30° was selected for further development.

Secondly, as a further improvement to reduce the back-face temperature to meet the design criteria of 453.15 K (180 °C) and below, the 30° carbon-phenolic material is augmented using a silica-phenolic material as the inner insulating material. For values measured up to 773.15 K (500 °C), the average thermal conductivity of the silica-phenolic material is 1/3.5 of that of the carbon-phenolic material used in this dual-layer ablator [13]. Silica-phenolic materials also have a history of being used as primary TPS materials, with two prominent examples being Aleastrasil, used in the European Space Agency's (ESA) Atmospheric Reentry Demonstrator (ARD) [14], and AQ60/I for the ESA's Huygens mission to Saturn's moon Titan [15]. A total of 12 dual-layer ablator specimens of different configurations were

tested using JBNU's 0.4 MW supersonic arc-jet plasma wind tunnel (PWT). The objectives of PWT tests were: a) to confirm that specimen silica-phenolic insulating layer internal temperatures meet the design limit of 453.15 K (180 °C) when exposed to the plasma test flow; b) to investigate how changes in recession layer thickness affect the specimen's internal temperatures; and c) to determine how much the specimen's stagnation temperature changes when the specimen's exposed surface changes from flat-faced to hemispherical-faced. The last two aspects will be useful for optimizing the ratio of the dual-layer ablator's recession layer to insulating layer thickness and the overall design of the actual spacecraft heat shield.

2. Methods

2.1. HVOF material ablation test facility

The HVOF material ablation test facility's torch [16,17], with a 10.84 mm flow exit diameter, is capable of generating high-velocity and high-temperature flows, to which both 0° and 30° carbon-phenolic material specimens were exposed. The specimens were tested at heat flux test conditions ranging from 3.25 to 11.5 MW/m^2. A two-colour pyrometer and an IR camera were used to measure each specimen's stagnation point temperature; with three K-type thermocouples used to measure each specimen's internal temperatures, at 10 mm (TC1), 20 mm (TC2), and 30 mm (TC3) from the specimen stagnation point. Fig. 1 shows the specimen dimensions for the HVOF tests.

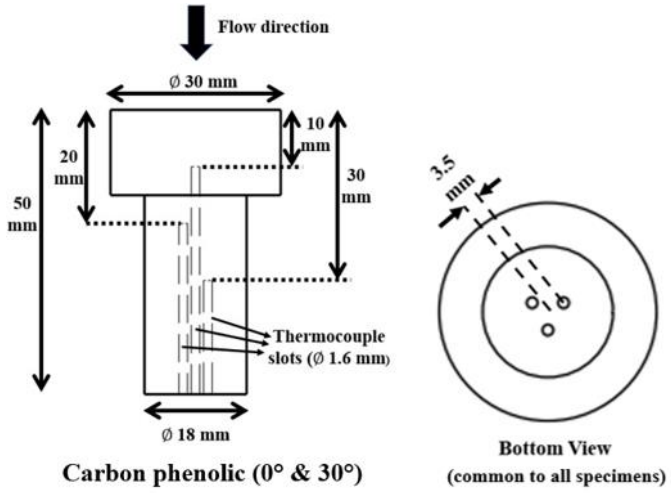

Fig 1. HVOF material ablation test specimen dimensions

Table 1 shows the HVOF specimen test conditions.

Table 1. HVOF specimen test conditions

No.	Specimen	Heat Flux (MW/m^2)	Test Duration (s)	Distance from the HVOF Nozzle Exit (mm)
1	CP (0°)-1	3.25	60	150
2	CP (0°)-3	6	30	120
3	CP (30°)-1	3.25	60	150
4	CP (30°)-2	6	30	120
5	CP (30°)-3	9	30	100
6	CP (30°)-4	11.5	30	90

CP (0°) = carbon-phenolic (0° lamination). CP (30°) = carbon-phenolic (30° lamination).

Before conducting HVOF specimen tests, the heat flux in the axial direction of the HVOF flow was measured using a water-cooled Gardon gauge. Similarly, a Gardon gauge heat flux measurement was also performed for the PWT test flow before conducting PWT specimen tests.

More details about the HVOF test experimental setup and specimen fabrication techniques can be found in [18].

2.2. 0.4 MW supersonic arc-jet PWT

Using JBNU's 0.4 MW supersonic arc-jet PWT [19,20], a total of 12 dual-layer ablator specimens were tested, with 6 being flat-faced and the remaining 6 being hemispherical-faced. Two different test conditions were used: 1) a stationary test condition of 7.5 MW/m^2 for 40 s, and 2) a transient test condition in which specimens while being exposed to the plasma test flow, moved from the location of 6.25 MW/m^2 to the location of 9.4 MW/m^2 and back in approximately 108 s. The transient test condition was designed to simulate the high-peak portion of an interplanetary spacecraft's re-entry heat flux trajectory, while the stationary test condition was used to measure the specimen's stagnation point temperatures, using a two-colour pyrometer, as the usage of the pyrometer is not possible when the specimens are in motion. The flat-faced specimens included three pairs, each pair with the same level of carbon-phenolic layer thickness. In each pair, one specimen was subjected to a stationary test, and the other was subjected to a transient test. The same arrangement was also applied to the hemispherical-faced specimens. For all specimens, internal temperatures were measured at 30 mm (inside the recession layer), at 20 mm (at the recession layer-insulating layer intersection), and at 10 mm (inside the insulating layer) from each specimen's bottom surface. The internal temperature measurements were conducted during the tests using K-type thermocouples. Fig. 2 shows the specimen dimensions for the PWT tests.

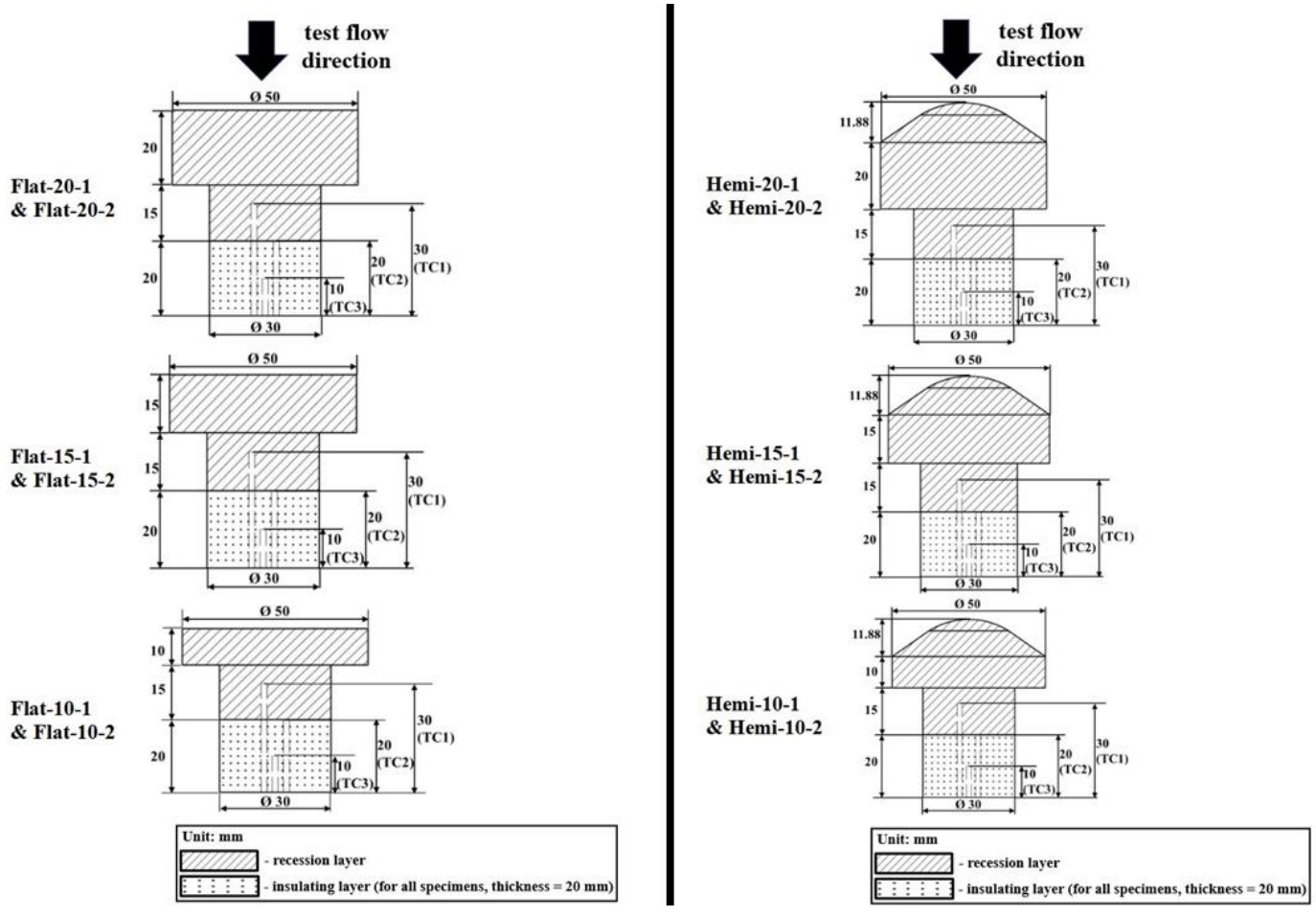

Fig 2. PWT specimen dimensions (left side: flat-faced specimens and right side: hemispherical-faced specimens)

Table 2 provides information on each specimen's test conditions, total length, recession layer thickness, and the locations of thermocouple measurements from the stagnation point.

Table 2. PWT specimen specifications

No.	Specimen	Exposed Surface Shape and Test Condition	Specimen Length or Thickness (mm)	Carbon-Phenolic Recession Layer Thickness (mm)	Thermocouple Measurement Location from Specimen Stagnation Point (mm)		
					TC1	TC2	TC3
1	Flat-20-1	Flat and stationary	55	35	25	35	45
2	Flat-20-2	Flat and transient					
3	Flat-15-1	Flat and stationary	50	30	20	30	40
4	Flat-15-2	Flat and transient					
5	Flat-10-1	Flat and stationary	45	25	15	25	35
6	Flat-10-2	Flat and transient					
7	Hemi-20-1	Hemispherical and stationary	66.88	46.88	36.88	46.88	56.88
8	Hemi-20-2	Hemispherical and transient					
9	Hemi-15-1	Hemispherical and stationary	61.88	41.88	31.88	41.88	51.88
10	Hemi-15-2	Hemispherical and transient					
11	Hemi-10-1	Hemispherical and stationary	56.88	36.88	26.88	36.88	46.88
12	Hemi-10-2	Hemispherical and transient					

For all specimens, silica-phenolic insulating layer thickness = 20 mm. For all specimens, TC1, TC2, and TC3 locations from the bottom surface were 30 mm, 20 mm, and 10 mm, respectively.

Table 3 shows the PWT specimen test conditions. More detailed information on PWT test experimental setup and specimen dimensions and construction can be found in [21] and the silica-phenolic material fabrication technique can be found in [13].

Table 3. PWT specimen test conditions

Test Condition	Heat Flux (MW/m^2)	Distance from the Torch Nozzle Exit (mm)	Duration (s)
Stationary	7.5	170	~40
Transient *	from 6.25 ± to 9.4	180 to 120	50
	9.4	120	~8 €
	from 9.4 to 6.25 ±	120 to 180	50

* Continuous exposure to the test flow, a total of ~108 s. ± Empirically estimated from experimental values measured using the Gardon gauge. € Average displacement mechanism direction reset time.

3. Results

3.1. HVOF tests

During the 0° carbon-phenolic specimen tests, periodic explosions were observed on the exposed surfaces of the tested specimens. These periodic explosions were abnormal and were not observed in the case of the 30° carbon-phenolic specimens. The lamination angle and inter-laminate pressure build-up during the tests are considered as reasons for the periodic surface explosions seen during the 0° carbon-phenolic specimen tests. Fig. 3 shows an explosion event that occurred during a 0° carbon-phenolic specimen test (CP (0°)-3).

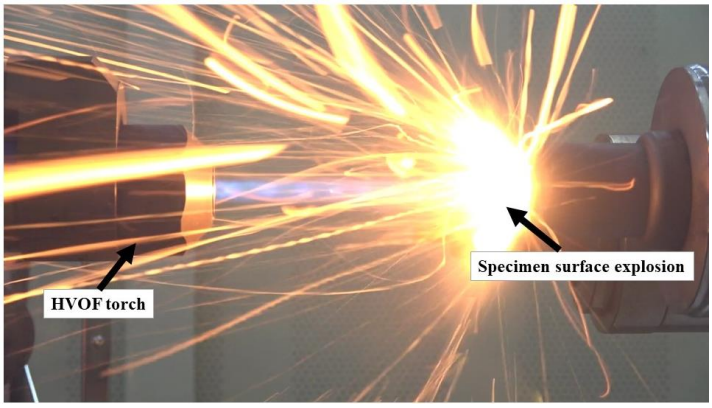

Fig 3. Explosion on CP (0°)-3 specimen surface during HVOF test

The surface temperature fluctuations caused by periodic surface explosions during the 0° carbon-phenolic specimen tests can be seen in Fig. 4. Fig. 4 shows that the intensity of surface temperature fluctuations (i.e., the periodic explosions on the specimen-exposed surface) increases with the heat flux.

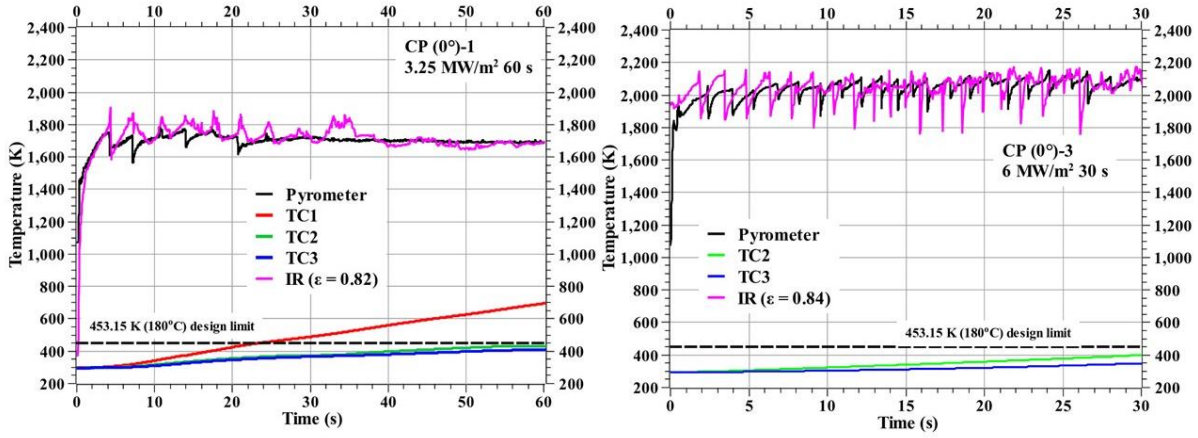

Fig 4. CP (0°)-1 and CP (0°)-3 temperature responses

In the case of 30° carbon-phenolic specimens, during the test at the lowest heat flux (3.25 MW/m^2 for 60 s), all measured internal temperatures exceeded the design limit of 453.15 K (180 °C) before the end of the test duration. In the higher heat flux tests (6 MW/m^2, 9 MW/m^2, and 11.5 MW/m^2, each lasting 30 s; it's important to note the shorter test duration), all internal temperatures, except those at 30 mm from the stagnation points exceeded the design limit of 453.15 K (180 °C) before the end of

the test duration. Fig. 5 and Fig. 6 show the temperature responses of the 30° carbon-phenolic specimens during the tests.

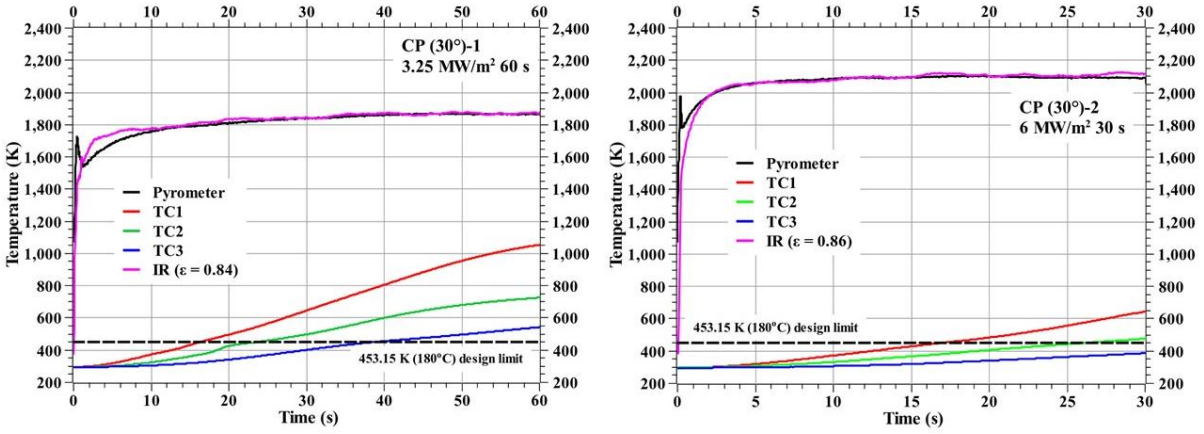

Fig 5. CP (30°)-1 and CP (30°)-2 temperature responses

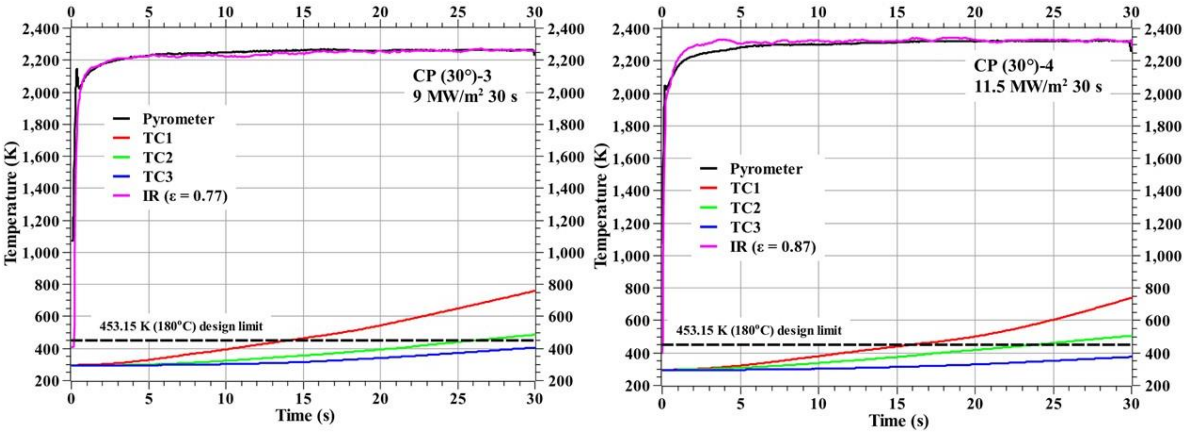

Fig 6. CP (30°)-3and CP (30°)-4 temperature responses

As an interplanetary ballistic spacecraft re-entry typically lasts approximately 100 s or more, the test results suggest that all internal temperatures, including those measured at 30 mm from the specimen stagnation points, would exceed the design limit when exposed for a longer duration. Table 4 shows the mass loss rate and recession rate for the HVOF test specimens.

Table 4. HVOF test mass loss rates and recession rates

No.	Specimen	Mass Loss Rate (g/s)	Recession Rate (mm/s)
1	CP (0°)-1	0.09	0.09
2	CP (0°)-3	0.17	0.12
3	CP (30°)-1	0.07	0.06
4	CP (30°)-2	0.11	0.10
5	CP (30°)-3	0.12	0.13
6	CP (30°)-4	0.13	0.15

The mass loss rate of surface recession, calculated using Eq. 1 and shown in Fig. 7, reveals that the trend of the 0° carbon-phenolic specimens is steeper compared to the 30° carbon-phenolic specimens. Therefore, due to this and because of the periodic explosion phenomenon observed during the 0° carbon-phenolic specimen tests, only the 30° carbon-phenolic material is selected and further augmented with silica-phenolic material, which has lower thermal conductivity, to form the dual-layer ablator. This is done to maintain the heat shield back face temperature below the design limit during the spacecraft re-entry phase.

$$mass\ loss\ rate\ of\ surface\ recession\ [g\ m^{-2}s^{-1}] = \frac{Recession\ [m]}{Test\ duration\ [s]} \times specimen\ density\ \left[\frac{g}{m^3}\right] \quad (1)$$

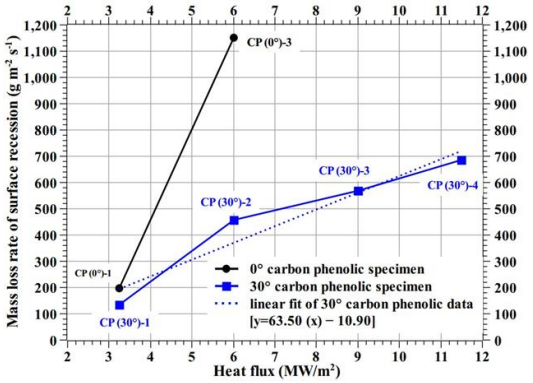

Fig 7. Mass loss rate of surface recession (HVOF tests)

A more detailed discussion about the HVOF experimental results can be found here [18].

3.2. PWT tests

During all specimen tests, regardless of the thickness and shape of the carbon-phenolic recession layer, the internal temperatures measured within the silica-phenolic insulating layers remained below 453.15 K (i.e., 180 °C) throughout the test durations, thereby satisfying the design criteria set for the dual-layer ablator. The hemispherical-faced specimens exhibited higher stagnation point temperatures than the flat-faced specimens, about 350 K higher, despite being tested at an identical heat flux condition. The average maximum stagnation point temperature for the hemispherical-faced specimens was approximately 2977 K, while for the flat-faced specimens, it was around 2628 K. The internal temperatures of the carbon-phenolic recession layers in the specimens showed that as the measuring point moved closer to the specimen's stagnation point, the carbon-phenolic internal temperature exhibited a more exponential rise. Fig. 8 shows the PWT test photographs.

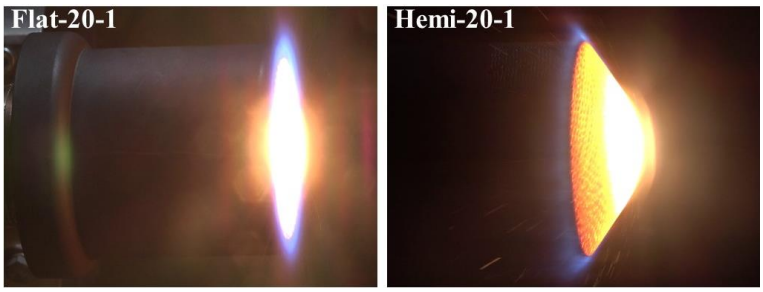

Fig 8. PWT test photographs (left side: Flat-faced specimen and right side: hemispherical-faced specimen)

Figs. 9-15 show the temperatures responses of the specimens during the PWT tests.

During the transient test of the hemispherical-faced specimen Hemi-20-2, it was observed that due to the specimen's shape, the plasma test flow was directed towards the graphite specimen holder, leading to the breakage of both the specimen and the holder. To avoid this issue, a specimen holder with a rectified design was used in the remaining two transient tests and all stationary tests of hemispherical-faced specimens. Additionally, due to the forementioned design issue with the specimen holder, the TC1 temperature of the Hemi-20-2 specimen was very close to the TC1 temperature of Hemi-15-2, despite the TC1 location of the Hemi-20-2 being 5 mm further away from the stagnation point compared to the TC1 location of Hemi-15-2.

During the stationary test of Hemi-15-1, a delay in exposure to the plasma test flow led to a sustainable increase in the specimen's internal temperatures prior to the test, due to the rise in the PWT test chamber's ambient temperature. This caused the TC2 and TC3 temperatures of the Hemi-15-1 specimen to exceed those of Hemi-10-1, a trend which continued throughout the test duration, even

though the TC2 and TC3 measuring locations of Hemi-15-1 were each 5 mm further away from the stagnation point when compared to the corresponding measuring locations of Hemi-10-1.

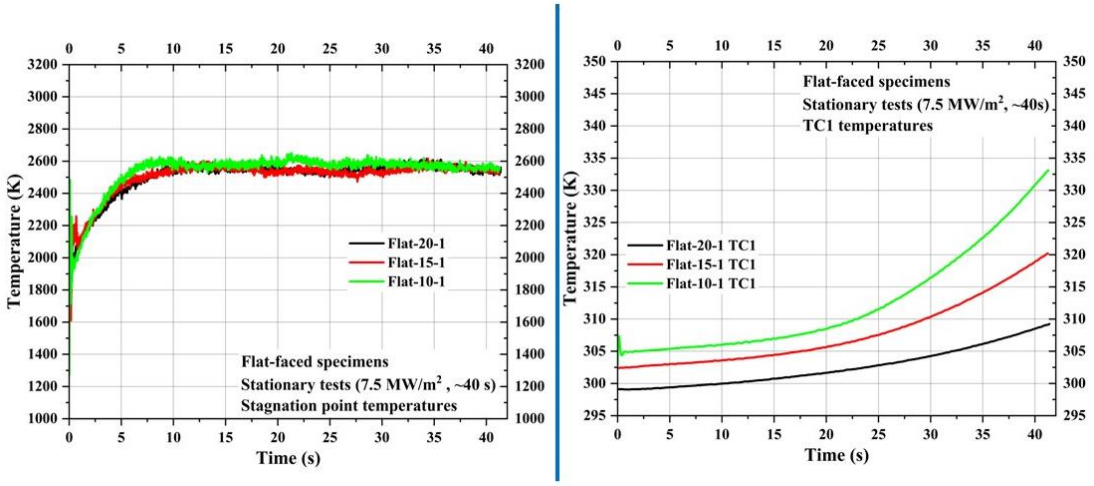

Fig 9. PWT test: Flat-faced specimen stationary tests stagnation point and TC1 temperatures

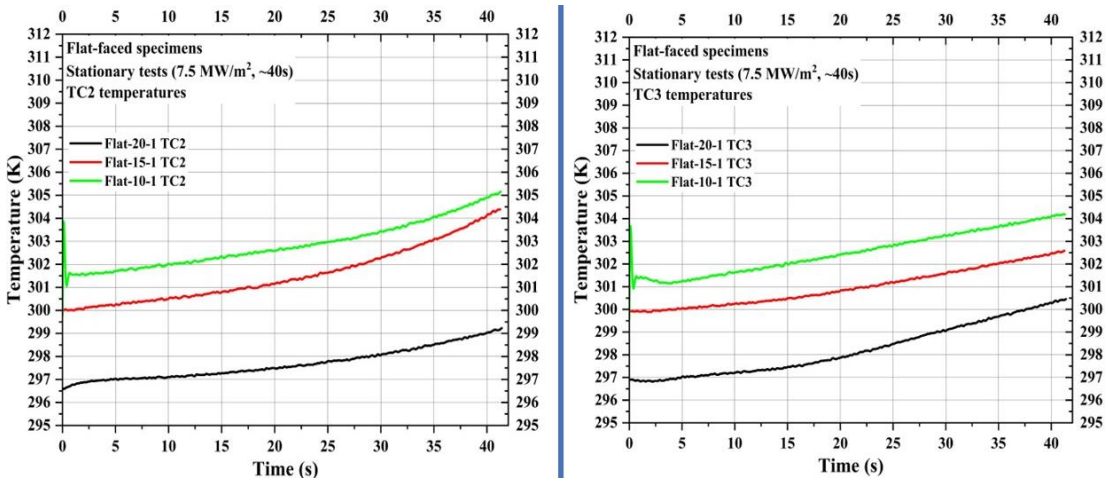

Fig 10. PWT test: Flat-faced specimen stationary tests TC2 and TC3 temperatures

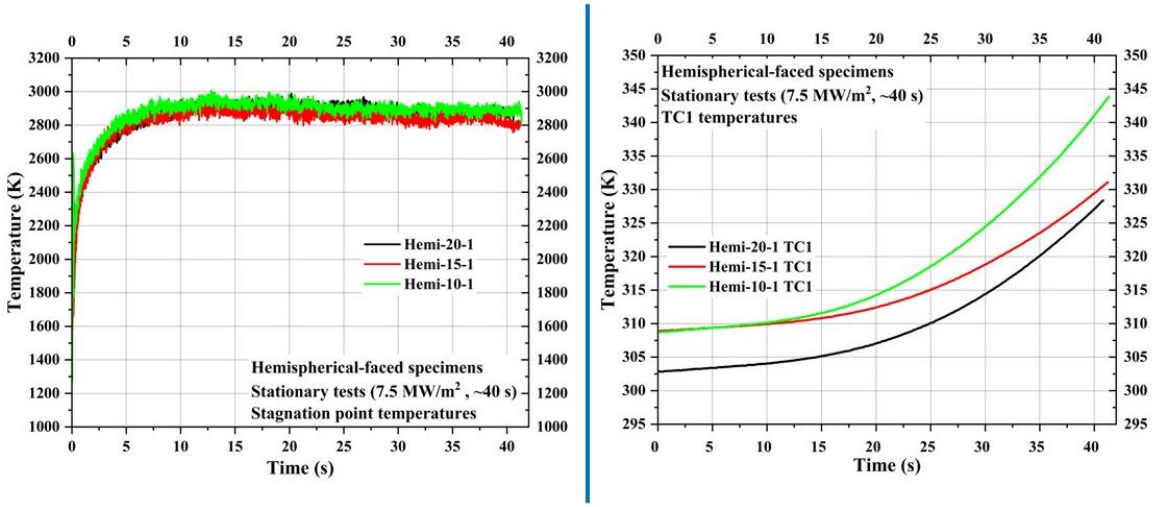

Fig 11. PWT test: Hemispherical-faced specimen stationary tests stagnation point and TC1 temperatures

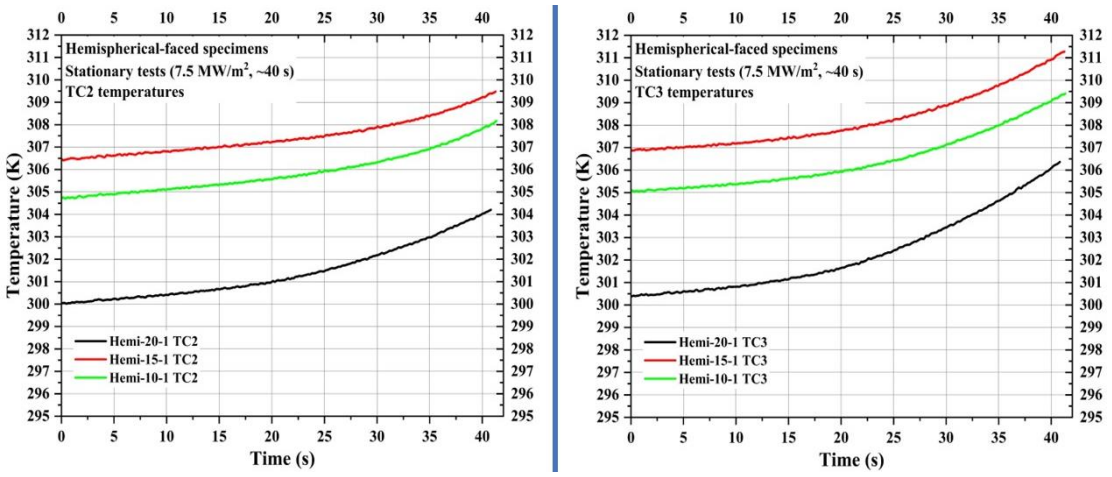

Fig 12. PWT test: Hemispherical-faced specimen stationary tests TC2 and TC3 temperatures

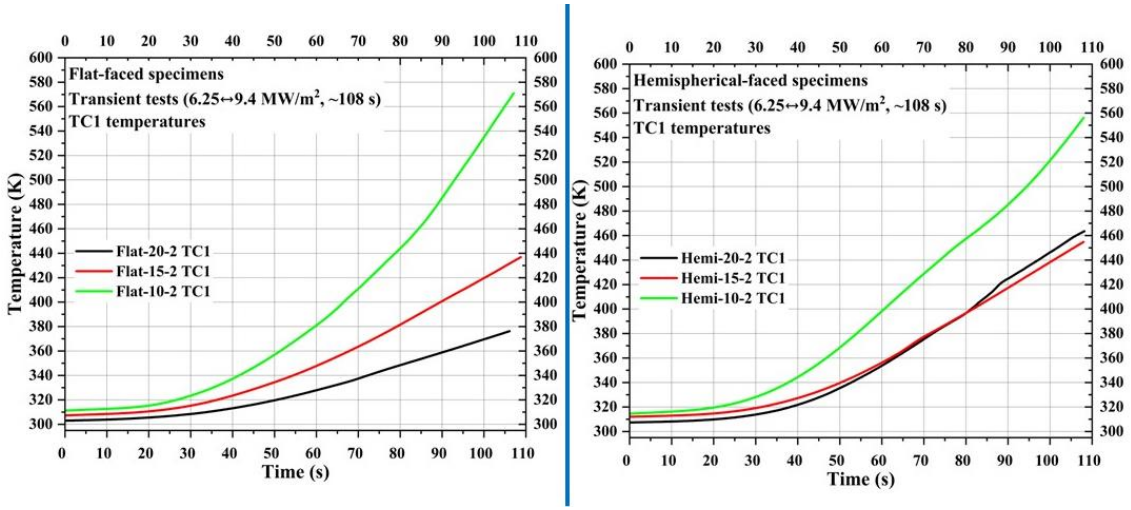

Fig 13. PWT test: Transient tests; flat-faced specimens TC1 and hemispherical specimens TC1 temperatures

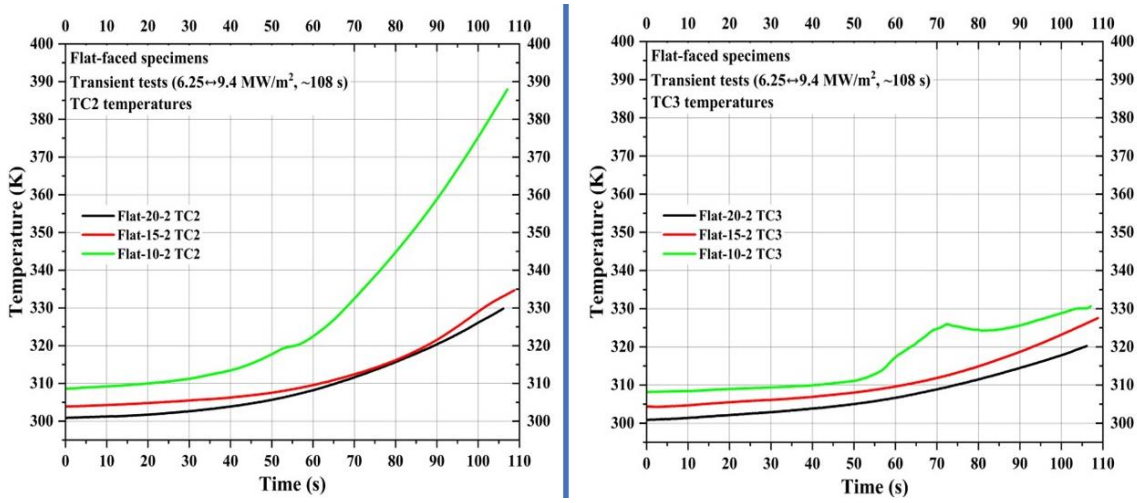

Fig 14. PWT test: Flat-faced specimen transient tests TC2 and TC3 temperatures

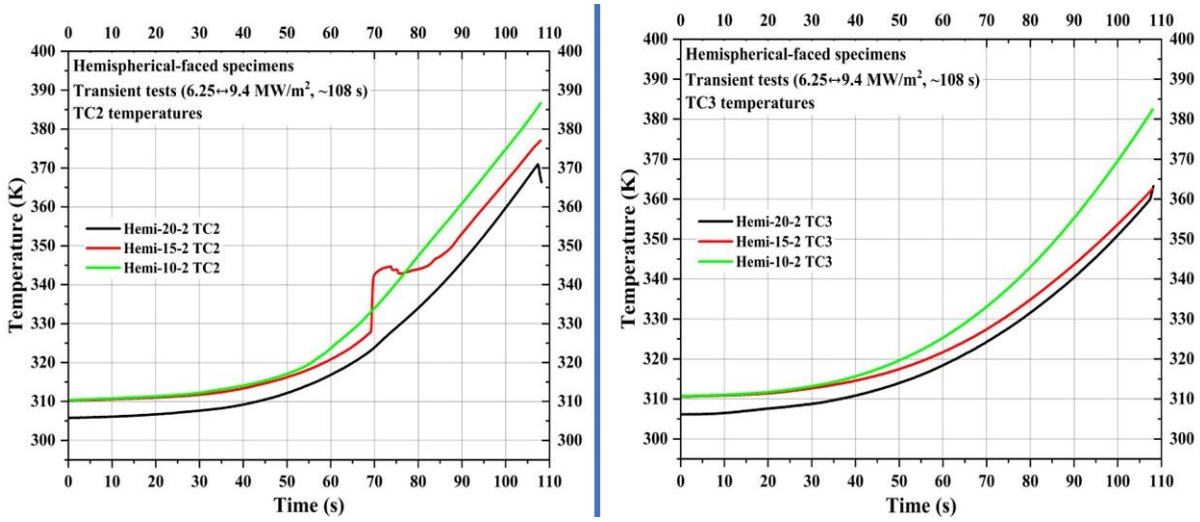

Fig 15. PWT test: Hemispherical-faced specimen transient tests TC2 and TC3 temperatures

When averaged, hemispherical-faced specimens exhibited approximately 1.4 times more mass loss and recession than the flat-faced specimens. The average recession rates were 0.05 mm/s for stationary flat-faced specimens, 0.07 mm/s for both transient flat-faced and stationary hemispherical faced specimens, and 0.09 mm/s for transient hemispherical-faced specimens, respectively. This data will be helpful in determining the overall design of the spacecraft's heat shield.

A more detailed discussion about the PWT experimental results can be found here [21].

4. Future works

In the future, a complete forebody heat shield for the Space Challenge Reentry Capsule (SCRC) will be constructed using the developed carbon-phenolic/silica-phenolic dual-layer ablator and will be tested by exposing it to rocket exhaust plume. Fig. 16 shows a mock-up of the SCRC.

Space Challenge Reentry Capsule (SCRC) mock-up

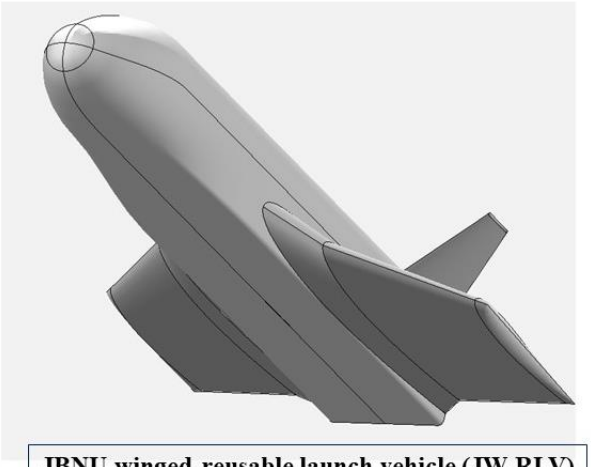

JBNU winged-reusable launch vehicle (JW-RLV) conceptual design

Fig 16. Space Challenge Reentry Capsule mock-up and JBNU winged-reusable launch vehicle conceptual design

Further, based on the expertise gained from the development of the dual-layer ablator, reusable TPS materials for a winged-reusable launch vehicle will be studied and developed. This study will also

include primary design development and trajectory estimation of the winged-reusable launch vehicle. Fig. 16 also shows the conceptual design of the winged-reusable launch vehicle.

5. Conclusion

A dual-layer ablator, composed of carbon-phenolic and silica-phenolic, is developed for the heat shield applications of an interplanetary Earth return spacecraft. This paper summarizes the testing methodologies involved in the development of the dual-layer ablator and highlights its ability to maintain its insulating layer temperature below 453.15 K (i.e., 180 °C) when exposed to extreme heat flux conditions.

Acknowledgement

The current research was supported by the Space Challenge Program funded by the Korea government (MSIT) (NRF-2022M1A3B8075123).

References

1. Laub B, Venkatapathy E Thermal protection system technology and facility needs for demanding future planetary missions. In: International Workshop Planetary Probe Atmospheric Entry and Descent Trajectory Analysis and Science, Lisbon, Portugal, 01/31 2004. pp 239-247

2. Pulci G, Tirillò J, Marra F, Fossati F, Bartuli C, Valente T (2010) Carbon–phenolic ablative materials for re-entry space vehicles: Manufacturing and properties. Composites Part A: Applied Science and Manufacturing 41 (10):1483-1490. doi:https://doi.org/10.1016/j.compositesa.2010.06.010

3. Curry DM (1993) Space Shutlle Orbiter Thermal Protection System Design and Flight Experience. NASA-TM-104773

4. Paglia L, Genova V, Tirillò J, Bartuli C, Simone A, Pulci G, Marra F (2021) Design of New Carbon-Phenolic Ablators: Manufacturing, Plasma Wind Tunnel Tests and Finite Element Model Rebuilding. Applied Composite Materials 28 (5):1675-1695. doi:10.1007/s10443-021-09925-8

5. Davies C, Arcadi M (2006) Planetary Mission Entry Vehicles Quick Reference Guide. Version 3.0. NASA/SP-2006-3401, NASA, Washington DC, USA

6. Yamada T, Inatani Y, Hirai Kc (2003) Thermal Responses of Ablator for Reentry Capsules with Superorbital Velocity The Institute of Space and Astronautical Science Report SP No 17, Sagamihara, Kanagawa, Japan

7. Shi S, Wang Y, Jiang T, Wu X, Tang B, Gao Y, Zhong N, Sun K, Zhao Y, Li W, Yu J (2022) Carbon Fiber/Phenolic Composites with High Thermal Conductivity Reinforced by a Three-Dimensional Carbon Fiber Felt Network Structure. ACS Omega 7 (33):29433-29442. doi:10.1021/acsomega.2c03848

8. Kaufman JG (2016) Fire Resistance of Aluminum and Aluminum Alloys and Measuring the Effects of Fire Exposure on the Properties of Aluminum Alloys ASM International®, OH, USA, p.2

9. Paglia L, Tirillò J, Marra F, Bartuli C, Simone A, Valente T, Pulci G (2016) Carbon-phenolic ablative materials for re-entry space vehicles: plasma wind tunnel test and finite element modeling. Materials & Design 90:1170-1180. doi:https://doi.org/10.1016/j.matdes.2015.11.066

10. Natali M, Torre L, Puri I, Rallini M (2022) Thermal degradation of phenolics and their carbon fiber derived composites: A feasible protocol to assess the heat capacity as a function of

temperature through the use of common DSC and TGA analysis. Polymer Degradation and Stability 195:109793. doi:https://doi.org/10.1016/j.polymdegradstab.2021.109793

11. Milos FS, Chen Y-K, Mahzari M (2018) Arcjet Tests and Thermal Response Analysis for Dual-Layer Woven Carbon Phenolic. Journal of Spacecraft and Rockets 55 (3):712-722. doi:10.2514/1.A34142

12. Park JS (2024) 전북대 최성만 교수팀, 국내 최초 지구 재진입 열 보호체 개발에 도전 (In English : Jeonbuk National University Professor Seong Man Choi's Team Takes on the Challenge of Developing the First Spacecraft Heat Shield for Earth Re-entry in South Korea): https://m.inews24.com/v/1675606. INEWS24. Accessed 2024.01.12

13. Chinnaraj RK, Kim YC, Choi SM (2023) Arc-Jet Tests of Carbon-Phenolic-Based Ablative Materials for Spacecraft Heat Shield Applications. Materials 16 (10):3717

14. Tran P, Paulat JC, Boukhobza P (2007) Re-entry Flight Experiments Lessons Learned – The Atmospheric Reentry Demonstrator. Flight Experiments for Hypersonic Vehicle Development (pp 10-1 – 10-46), Educational Notes RTO-EN-AVT-130, Paper 10 Neuilly-sur-Seine, France

15. Bouilly J-M Thermal Protection of the Huygens Probe During Titan Entry: Last Questions. In: 2nd International Planetary Probe Workshop; 113-120; NASA/CP-2004-213456, Moffett Field, CA, USA, 2005.

16. Chinnaraj RK, Hong SM, Kim HS, Choi SM (2023) Ablation Experiments of High-Temperature Materials (Inconel, C–C and SiC) Using a High-Velocity Oxygen-Fuel Torch. International Journal of Aeronautical and Space Sciences 24 (2):321-333. doi:10.1007/s42405-022-00514-y

17. Chinnaraj RK (2022) Supersonic High Temperature Flow Diagnosis and Material Ablation Experiments Using the HVOF System PhD Dissertation. Jeonbuk National University, Jeonju, Republic of Korea

18. Chinnaraj RK, Kim YC, Choi SM (2023) Thermal Ablation Experiments of Carbon Phenolic and SiC-Coated Carbon Composite Materials Using a High-Velocity Oxygen-Fuel Torch. Materials 16 (5):1895

19. Tekna Plasma Systems Inc., 0.4MW Class Enhanced Huels Type Plasma System. Operating Manual – System 93, Sherbrooke, Quebec, Canada

20. Chinnaraj RK, Oh PY, Shin ES, Hong BG, Choi SM (2019) Mach Number Determination in a High-Enthalpy Supersonic Arc-Heated Plasma Wind Tunnel. International Journal of Aeronautical and Space Sciences 20 (1):70-79. doi:10.1007/s42405-018-0128-x

21. Chinnaraj RK, Kim YC, Choi SM (2023) Thermal Behavior of Carbon-Phenolic/Silica Phenolic Dual-Layer Ablator Specimens through Arc-Jet Tests. Materials 16 (17):5929